Systems Science and Informatics Unit (SSIU)
Indian Statistical Institute, Bangalore
India

ESIEE
University of Paris-Est
France

19-22 October 2010
Bangalore

TERRESTRIAL ANALYSIS PART-I

1

SCALING AND MORPHOLOGIC ANALYSES OF TOPSAR DEMs: A QUANTITATIVE CHARACTERISATION PERSPECTIVE

B. S. Daya Sagar

2

Outline

- Data used: TOPSAR DEMs, simulated DEM
- Mathematical Morphological Transformations Employed include: Morphological Skeletonization, Recursive Morphological Pruning (Hit-or-Miss Transformation, Morphological Thinning etc), Morphological Reconstruction.
- For
  - Networks' extraction and their properties
  - Analyses via existing morphometric and allometric power-laws
  - Analyses via scaling relationships between travel-time channel networks, convex hulls and convexity measures
  - Analysis via Fractal and multiscale analyses of planar geophysical networks
- Conclusions

3

Mathematical Morphology (MM)

- Mathematical morphologic transformations (Matheron, 1975; Serra, 1982) have shown its speciality and strength in the context of geomorphology such as significant geomorphologic features extraction, basic measures of water bodies estimation, geomorphic processes modelling and simulation, fractal landscapes generation, etc.
- In the entire investigation, both DEM's are analysed as grey-scale image (3-D) and the extracted networks as thresholded sets (binary form).
- In order to process the binary sets such as channel networks, binary morphological transformations are employed.
- Grey-scale mathematical morphological transformations are used to process the three-dimensional images such as DEM's.
- The geometrical and topological structures of DEM are examined by matching it with structuring elements of various shapes and sizes at different locations in the DEM.
- Figure below provides two examples of structuring elements (*B*), which are in the shape of rhombus and square of size 3X3. (1's and 0's stand for foreground and background regions, respectively).

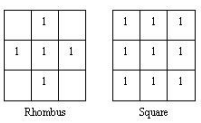

4

Mathematical Morphology (cont)

Binary MM

- Binary erosion transformation of S by structuring element, B
  - the set of points s such that the translated Bs is contained in the original set S, and is equivalent to intersection of all the translates.
  - $\boldsymbol{S \ominus B = \{s: B_s \subseteq S\}=} \bigcap_{b \in B} S_{-B}$
- Binary dilation transformation of S by B
  - the set of all those points s such that the translated Bs intersects S, and is equivalent to the union of all translates.
  - $\boldsymbol{S \oplus B = \{s: B_s \cap S \neq \emptyset\} =} \bigcup_{b \in B} S_{-B}$
- The dilation with an elementary structuring template expands the set with a uniform layer of elements, while the erosion operator eliminates a layer from the set.
- Multiscale erosions and dilations are

  - $(S \ominus B) \ominus B \ominus \ldots \ominus B = (S \ominus nB)$,

  - $(S \oplus B) \oplus B \oplus \ldots \oplus B = (S \oplus nB)$,

  where $nB = B \oplus B \oplus \ldots \oplus B$ and n is the number of transformation cycles.

5

Mathematical Morphology (cont)

Binary MM (cont)

- By employing erosion and dilation of S by B, opening and closing transformations are further represented as:
  - $S \circ B = ((S \ominus B) \oplus B))$
  - $S \bullet B = ((S \oplus B) \ominus B))$
- After eroding S by B, the resultant eroded version is dilated to achieve the opened version of S by B.
- Similarly, closed version of S by B is obtained by first performing dilation on S by B and followed by erosion on the resultant dilated version.
- Multiscale opening and closing transformations are implemented by performing erosions and dilations recursively as shown below.

  - $(S \circ nB) = [(S \ominus nB) \oplus nB)]$,

  - $(S \bullet nB) = [(S \oplus nB) \ominus nB)]$,

  where n is the number of transformations cycles.

6

Mathematical Morphology (cont)

Grey-scale MM

- Grey-scale dilation and erosion operations - expansion and contractions respectively
- Let $f(x,y)$ be a function on Z^2, and B be a fixed structuring element of size one. The erosion of DEM, $f(x)$ by B replaces the value of f at a pixel (x, y) by the minima values of the image in the window defined by the structuring template B
  - $(f \ominus B)(x,y) = \min_{(i,j)\in B} \{f(x+i, y+j)\}$,
- The dilation of DEM, $f(x)$ by B replaces the value of f at a pixel (x, y) by the maxima values of the image in the window defined by the structuring template B
  - $(f \oplus B)(x,y) = \max_{(i,j)\in B} \{f(x-i, y-j)\}$,
- In other words, $(f \ominus B)$ and $(f \oplus B)$ can be obtained by computing *minima* and *maxima* over a moving template B, respectively.
- Erosion is the dual of dilation :
  - Eroding foreground pixels is equivalent to dilating the background pixels.

7

Mathematical Morphology (cont)

Grey-scale MM (cont)

- Opening and closing are both based on the dilation and erosion transformations.
- Opening of DEM, f by B is achieved by eroding f and followed by dilating with respect to B, $(f \circ B) = [(f \ominus B) \oplus B]$,
- Closing of f by B is defined as the dilation of f by B followed by erosion with respect to B, $(f \bullet B) = [(f \oplus B) \ominus B]$,
- Opening eliminates specific image details smaller than B, removes noise and smoothens the boundaries from the inside, whereas closing fills holes in objects, connects close objects or small breaks and smoothens the boundaries from the outside.
- Multiscale opening and closing can be performed by increasing the size (scale) of the structuring template Bn, where n = 0, 1, 2,…, N. These multiscale opening and closing of f by B are mathematically represented as:
  $(f \circ B_n) = \{[(f \ominus B) \ominus B \ominus \ldots \ominus B] \oplus B \oplus B \oplus \ldots \oplus B\} = [(f \ominus nB) \oplus nB]$,
  $(f \bullet B_n) = \{[(f \oplus B) \oplus B \oplus \ldots \oplus B] \ominus B \ominus B \ominus \ldots \ominus B\} = [(f \oplus nB) \ominus nB]$,
  at scale n = 0, 1, 2,…, N.
- Performing opening and closing iteratively by increasing the size of B transforms the DEM into lower resolutions correspondingly.

8

Mathematical Morphology (cont)

- Multiscale opening and closing of DEM by *nB* effect spatially distributed elevation regions in the form of smoothing of contours to various degrees. The shape and size of *B* control the shape of smoothing and the scale respectively.
- Important problems like feature detection and characterisation often require analysing DEMs at multiple spatial resolutions. Recently, non-linear filters have been used to obtain images at multi-resolution due to their robustness in preserving the fine details.
- Advantages of mathematical morphology transformations
  - popular in object recognition and representation studies.
  - The non-linearity property in preserving the fine details.

9

Basic Transformations

- Mathematical Morphology
  - Dilation
  - Erosion
  - Opening
  - Closing
- Fractals

10

Effect of Dilation using 3X3 structuring element

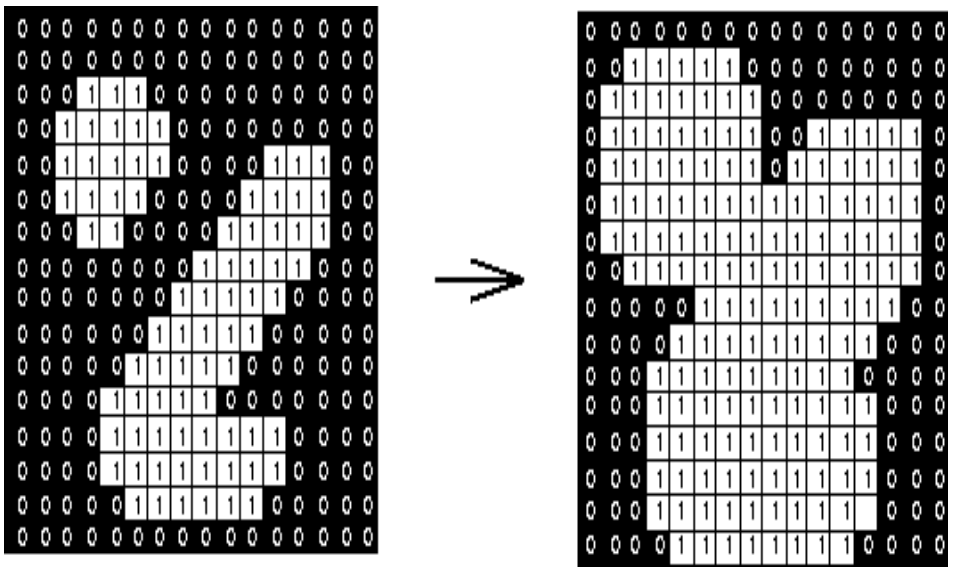

11

Steps in Dilation of C by S

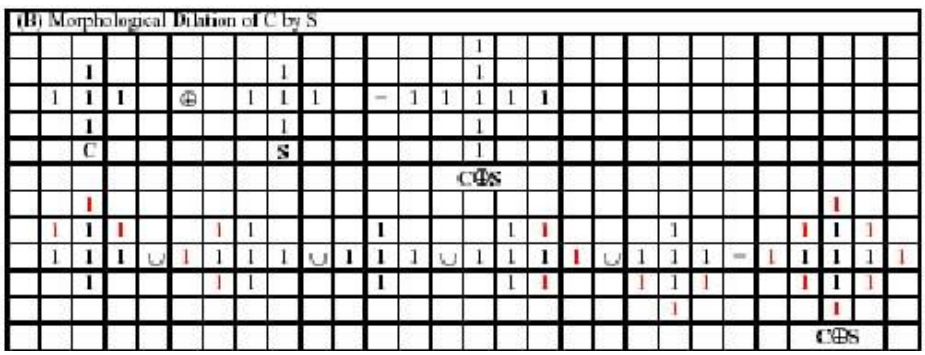

12

Effect of Erosion using 3X3 structuring element

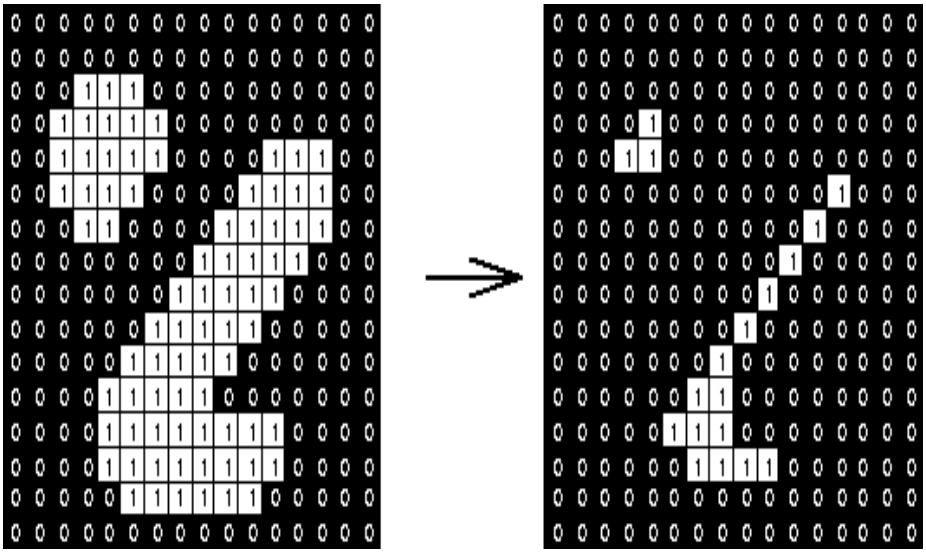

13

Steps in Erosion of C by S

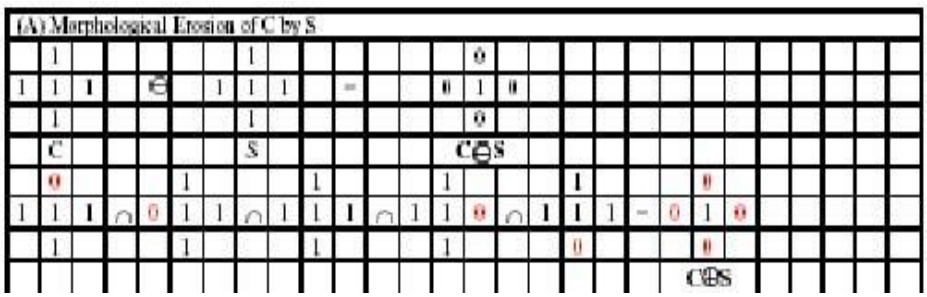

14

Effect of Opening using 3X3 structuring element

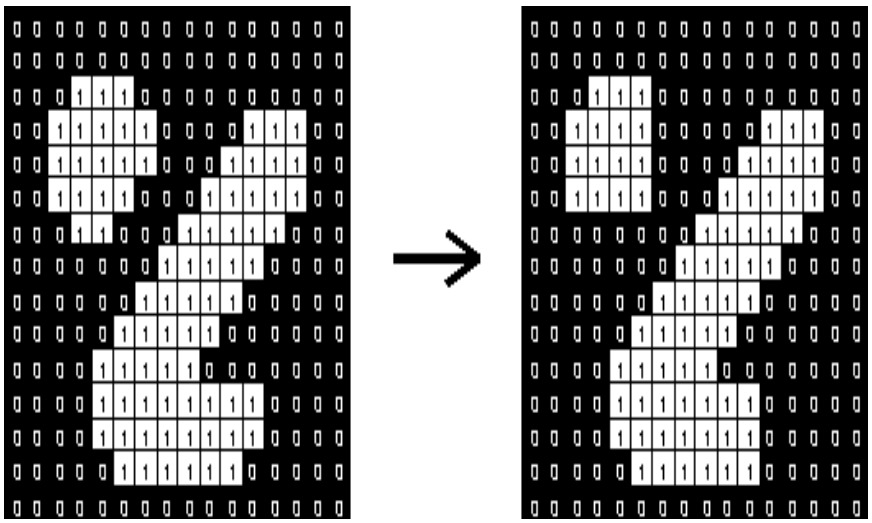

15

Steps in Opening of C by S

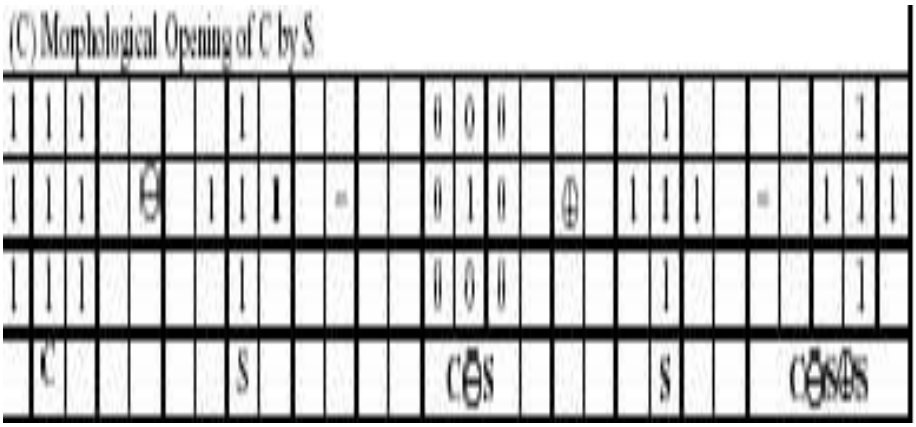

16

Effect of Closing using 3X3 structuring element

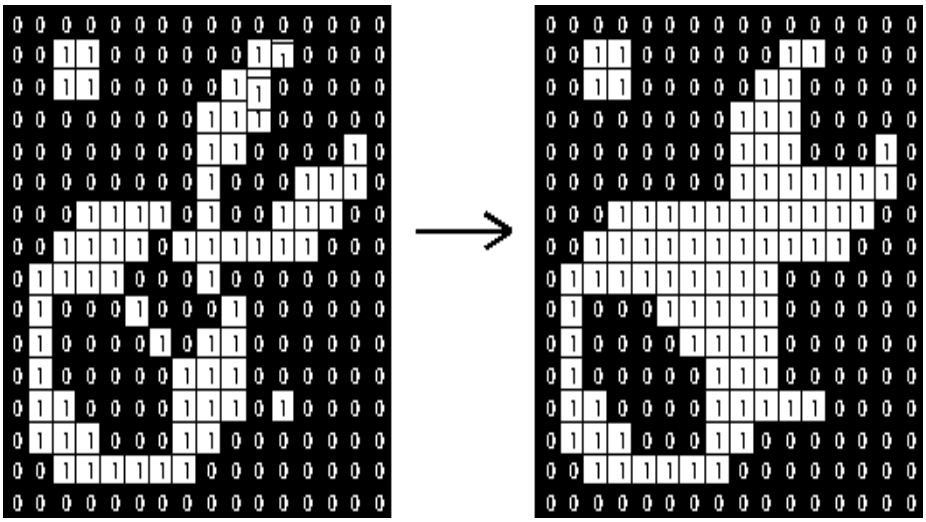

17

Steps in Closing of C by S

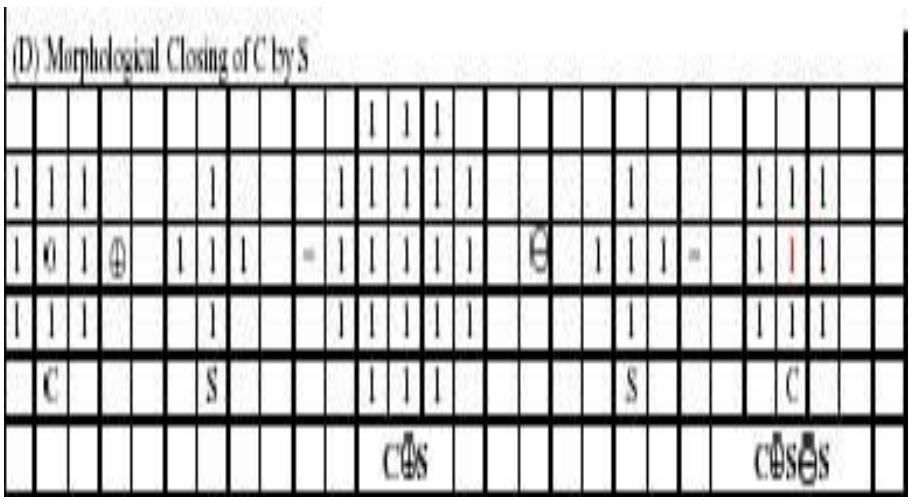

18

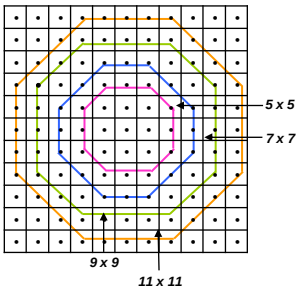

Octagonal symmetric structuring elements of various primitive sizes ranging from 5 × 5 to 11 × 11. These primitive sizes can be considered as B.

Multiscale Opening and Closing

$$M \circ nB = \{[(M \ominus B) \ominus B \ldots \ominus B] \oplus B \oplus B \ldots \oplus B\} = [(M \ominus nB) \oplus nB]$$
$$M \bullet nB = \{[(M \oplus B) \oplus B \ldots \oplus B] \ominus B \ominus B \ldots \ominus B\} = [(M \oplus nB) \ominus nB]$$

- Multiscale grayscale transformations (erosion, dilation, opening, and closing), at scale n = 0,1,2,…,N, are defined as follows:

$$(f \ominus nB) = (f \ominus B) \ominus B \ominus B \ominus \ldots \ominus B$$

$$(f \oplus nB) = (f \oplus B) \oplus B \oplus B \oplus \ldots \oplus B$$

$$(f \circ nB) = [(f \ominus nB) \oplus nB]$$
$$(f \bullet nB) = [(f \oplus nB) \ominus nB]$$

Study area specification

♦ SPOT X-Band data of Machap Baru reservoir situated in Melaka state, Malaysia with spatial resolution of 20 m acquired on 28/2/1998 situated in between 2^{o} 15’ - 2^{o}25’ N. Latitude and 102^{o} 15’ - 102^{o} 23’ E.Longitude.

♦ Surveyed topographic map of scale 1:50000 for the region Machap Baru and Gunung Ledang.

♦ Data collected from Department of Irrigation and Drainage.

21

TOPSAR DEM

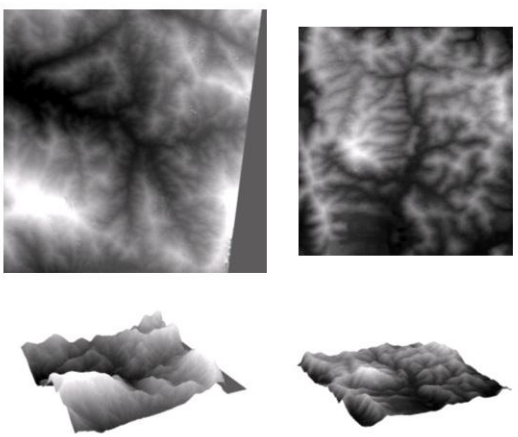

22

Study region 1: Cameron Highlands

- Cameron Highlands region is located in the eastern part of Perak state in Peninsular Malaysia.
- Location – 101^{o}15’-101^{o}20’ East longitudes and 4^{o}31’-4^{o}36’ North latitudes.
- The physical relief of this area is rough where it comprises a series of mountainous forest at altitudes between 400m and 1800m.

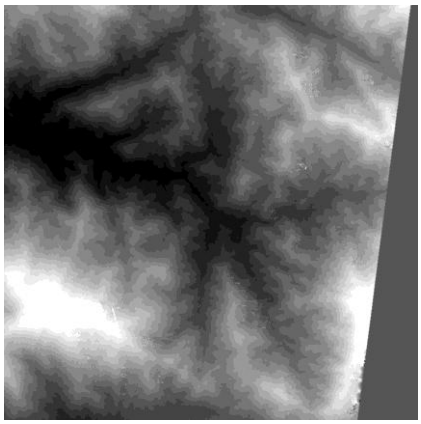

23

Study region 2: Petaling

- Petaling region is located in the southern part of Selangor state in Peninsular Malaysia.
- Location - 104^{o}09’-104^{o}13’ East longitudes and 2^{o}48’-2^{o}53’ North latitudes.
- This region is a relatively flat terrain with altitude from 27m to highest altitude of 215m.

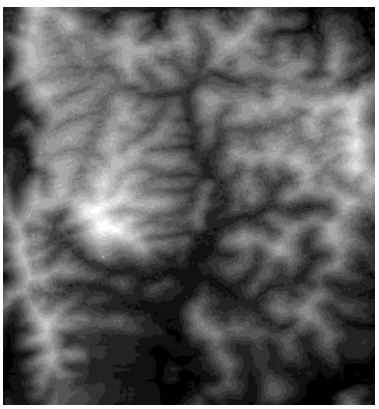

24

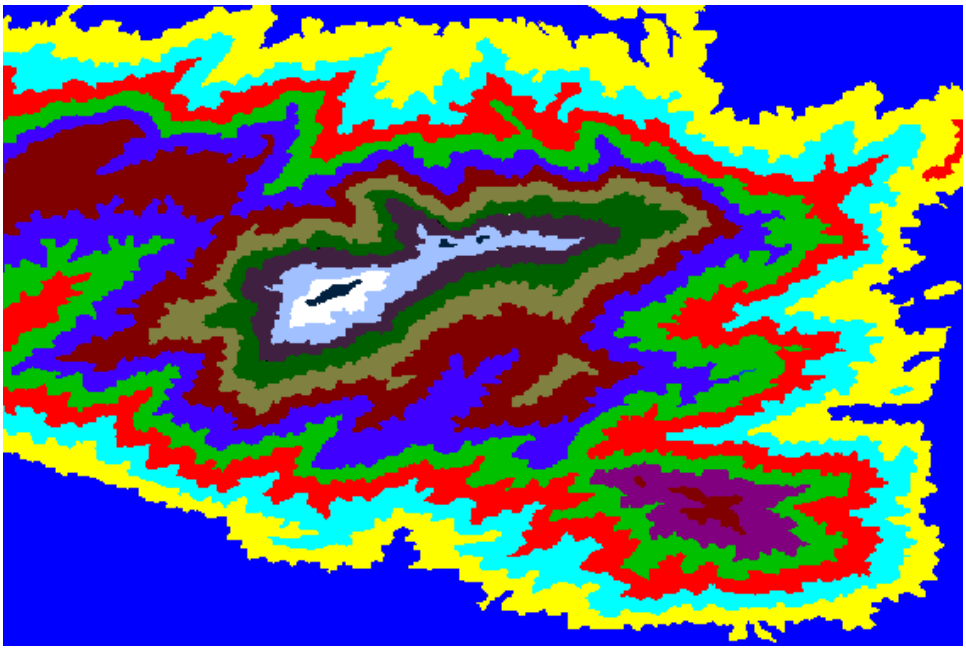

DEM of Gunung Ledang region

25

Simulated DEM

- The Hortonian fractal DEM, *M* is simulated by considering a binary fractal basin (*X*) that possesses 1s and 0s representing topological space of the basin and its complement, respectively.
- This binary fractal basin is decomposed into topologically prominent regions (TPRs) by employing morphological erosions, dilations, and logical difference and union operations to simulate fractal DEM (F-DEM). The simulation of internal topology of the basin within a defined geometric boundary is mathematically defined by

$$M = \bigcup_{n=0}^{N} \{\{(X \ominus nB) \setminus \{[(X \ominus nB) \ominus B] \oplus B\}\} \oplus nB\}$$

where, *X* is binary basin, *B* is structuring element that gets translated over *X*, and *n* is the size of this *B*. *X**Y* is the part of *X* that is not in *Y*. *X* and *S* are sets in Euclidean space with elements *x* and *s*, respectively, $x = (x_1,..., x_N)$ and $s = (s_1,..., s_N)$.

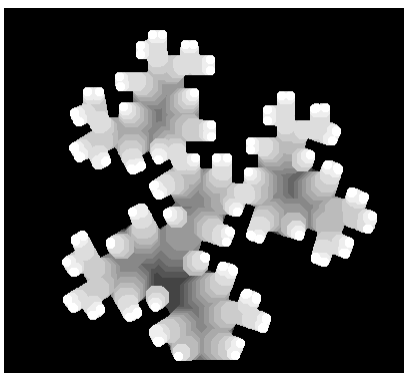

The symmetric octagon used as structuring element, *B* in this simulation.

26

Simulated DEM (cont)

Five main steps involved in the simulation are:

i. Successive erosion frontlines are generated *via* $(X \ominus nB)$ by increasing the size of structuring element. Erosions are performed iteratively to generate erosion frontlines within a binary fractal basin.

ii. Smoothening of the erosion frontlines is achieved *via* $(X \ominus nB) \ominus B]_{\oplus} B$. Here, the dilation combines the eroded version of the eroded binary basin achieved at step (i).

iii. Various orders of network subset ranging from n=0 to N are isolated from each erosion frontline by subtracting the resultant information achieved in step (ii) from step (i).

iv. TPRs are generated by dilating the resultant information, which is achieved at step (iii) by nB. This is an iterative procedure till the whole basin is converted into TPRs. Each TPR is assigned a specific value assuming that the spatially distributed TPRs are akin to spatially distributed elevation regions, and

v. Various orders of coded TPRs are combined to produce the simualted DEM. By employing these sequential steps, a self-affine fractal DEM is generated.

27

Simulated DEM

♦ Such an algorithm can be performed on a gray-level DEM or on the Threshold Decomposed Elevation Regions (TDER) of a DEM

♦ A simulated DEM with three spatially distributed elevation regions numerically represented as 1s, 2s and 3s

♦ Its Threshold Decomposed Elevation Regions are also represented.

♦ This Algorithm can be performed on individual TDERs to achieve channel and ridge connectivity network.

28

Synthetic DEM

1	1	1	1	1	1	1	1	1	1	1
1	2	2	2	2	2	2	2	2	2	1
1	2	2	2	2	2	2	2	2	2	1
1	2	2	3	3	3	3	3	2	2	1
1	2	2	3	3	3	3	3	2	2	1
1	2	2	3	3	3	3	3	2	2	1
1	2	2	3	3	3	3	3	2	2	1
1	2	2	3	3	3	3	3	2	2	1
1	2	2	2	2	2	2	2	2	2	1
1	2	2	2	2	2	2	2	2	2	1
1	1	1	1	1	1	1	1	1	1	1

29

TDER with T =1

1	1	1	1	1	1	1	1	1	1	1
1	1	1	1	1	1	1	1	1	1	1
1	1	1	1	1	1	1	1	1	1	1
1	1	1	1	1	1	1	1	1	1	1
1	1	1	1	1	1	1	1	1	1	1
1	1	1	1	1	1	1	1	1	1	1
1	1	1	1	1	1	1	1	1	1	1
1	1	1	1	1	1	1	1	1	1	1
1	1	1	1	1	1	1	1	1	1	1
1	1	1	1	1	1	1	1	1	1	1
1	1	1	1	1	1	1	1	1	1	1

30

TDER with T =2

0	0	0	0	0	0	0	0	0	0	0
0	1	1	1	1	1	1	1	1	1	0
0	1	1	1	1	1	1	1	1	1	0
0	1	1	1	1	1	1	1	1	1	0
0	1	1	1	1	1	1	1	1	1	0
0	1	1	1	1	1	1	1	1	1	0
0	1	1	1	1	1	1	1	1	1	0
0	1	1	1	1	1	1	1	1	1	0
0	1	1	1	1	1	1	1	1	1	0
0	1	1	1	1	1	1	1	1	1	0
0	0	0	0	0	0	0	0	0	0	0

31

TDER with T =3

0	0	0	0	0	0	0	0	0	0	0
0	0	0	0	0	0	0	0	0	0	0
0	0	0	0	0	0	0	0	0	0	0
0	0	0	1	1	1	1	1	0	0	0
0	0	0	1	1	1	1	1	0	0	0
0	0	0	1	1	1	1	1	0	0	0
0	0	0	1	1	1	1	1	0	0	0
0	0	0	1	1	1	1	1	0	0	0
0	0	0	0	0	0	0	0	0	0	0
0	0	0	0	0	0	0	0	0	0	0
0	0	0	0	0	0	0	0	0	0	0

←

32

Channel & Ridge networks

1					2					1
	1				2				1	
		1			2			1		
			1		2		1			
				1	2	1				
2	2	2	2	2	1	2	2	2	2	2
				1	2	1				
			1		2		1			
		1			2			1		
	1				2				1	
1					2					1

33

Networks extraction and their properties

34

Networks extraction and their properties

- The two topologically significant networks, i.e. channel and ridge networks are the abstract structures of concave and convex zones of the DEM's respectively.
- The paths of these extracted networks are the crenulations in the elevation contours.
- These crenulations can be isolated from DEM's by using nonlinear morphological transformations. These isolated crenulations form the ridge and channel networks.
- Basic morphological operators (i.e. erosion, dilation, opening and closing) are used in networks extraction.
- The DEM, *f* is first eroded by structuring element, B_n with *n*=1, 2,…,*N*, and the eroded DEM is opened by *B* of the smallest size. B_n is the increasing version of B_1 for *n*=1, 2, 3,…,*N*. The opened version of each eroded image is subtracted from the corresponding eroded image to produce the *n*th level subsets of the ridge network. Union of these subsets of level *n* = 0 to *N* gives the ridge network for the DEM.
- Ridge network

$$\mathrm{RID}_n^i(f) = [(f \ominus \mathrm{B}_n^i) \setminus \{[(f \ominus \mathrm{B}_n^i) \ominus \mathrm{B}_1^i] \oplus \mathrm{B}_1^i\}]$$

$$\mathrm{RID}(f) = \bigcup_{\substack{n=0 \\ i=1}}^{\substack{4 \\ N}} [\mathrm{RID}_n^i(f)]$$

35

Networks extraction and their properties

- Duality of the morphology approach is proposed for channel networks extraction. DEM, *f* is first dilated by structuring element, B_n and the dilated DEM is closed by structuring element, *B*, of the smallest size. The closed version of each dilated image is subtracted from the corresponding dilated image to produce the *n*th level subsets of the channel network. Union of these subsets of level *n* = 0 to *N* gives the channel network for the DEM.
- Channel network

$$\mathrm{CH}_n^i(f) = [(f \oplus \mathrm{B}_n^i) \setminus \{[(f \oplus \mathrm{B}_n^i) \oplus \mathrm{B}_1^i] \ominus \mathrm{B}_1^i\}]$$

$$\mathrm{CH}(f) = \bigcup_{\substack{n=0 \\ i=1}}^{\substack{4 \\ N}} [\mathrm{CH}_n^i(f)]$$

- Structuring elements of line segment as shown in figure below are used for B_1. Line segments in 4 different orientations are used as their shapes match the ridge and channel networks closely.
- The extracted networks are converted into binary form by using thresholding process. Morphological thinning approach is used to thin the network by reducing all lines to one-pixel wide thickness.

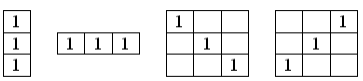

36

Algorithm

- An Algorithm is developed to extract singular networks such as channel and ridge connectivity networks from contour based DEM of Gunung Ledang region.
- Sub watershed boundary in DEM is automatically generated by considering channel and ridge connectivity networks and steepest descent property.
- Mathematical morphology transformations such as dilation, erosion, opening and closing are used in this algorithm to make it user-friendly.

37

Steps in Algorithm

- The following 5 step algorithm is used to extract two topological connectivity networks

Step1:

$$CH_e(M) = \epsilon_s^e(M) \cup \gamma_s^1\{\epsilon_s^e(M)\}$$
$$e = 0,1,2,\ldots,N$$

Step 2:

$$CH(M) = \bigcup_{e=0}^{N} CHe(M)$$
$$e = 0,1,2,\ldots,n$$

38

Steps in Algorithm

Step3:

$$RID_e(M) = \varepsilon^{e}_{s}((CH(M))^{c}) \,//\, \gamma^{1}_{s}(\varepsilon^{e}_{s}((CH(M))^{c}))$$

→

Step 4:

$$RID(M) = \bigcup_{e=1}^{N} RID_e(M)$$

$$e = 0, 1, 2, \ldots\ldots, n$$

Step 5:

$$CH(M) \cup RID(M)$$

39

DEM of Gunung Ledang with 8 sub watershed partition

40

J. Serra, J. Cousty, B. S. Daya Sagar
ISI, Univ Paris-Est

Automatic generation of sub watersheds from Digital Elevation Model

Digital Elevation Model (DEM) Generation:

♦ Contours produced from Topographic map of Gunung Ledang region.

♦ Assign unique colors to each contour interval

41

DEM of sub watershed and its boundary

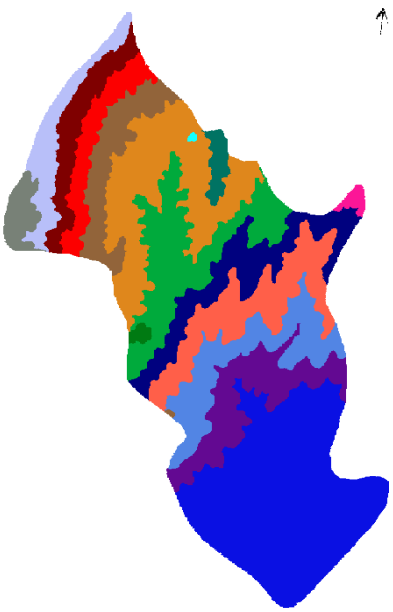

42

Channel and ridge networks

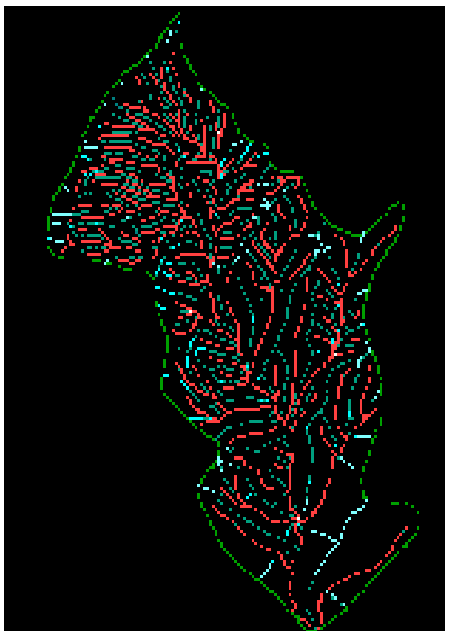

♦ ***Using Algorithm, channel network (red colour) and ridge network (cyan colour) are extracted automatically.***

43

Automatically generated sub watershed map

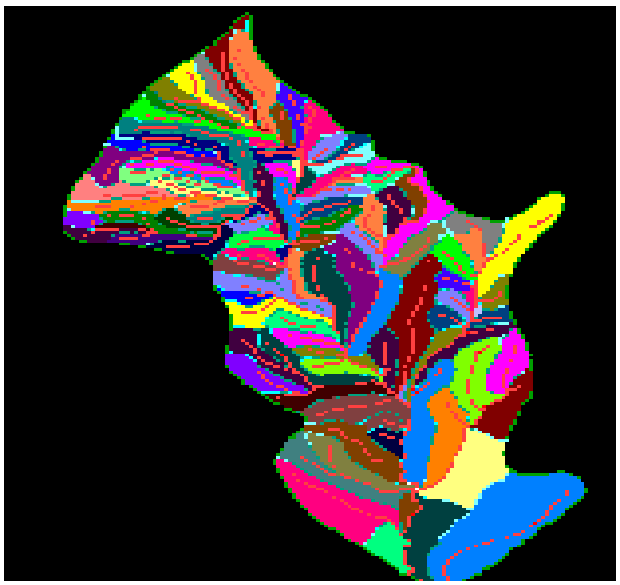

44

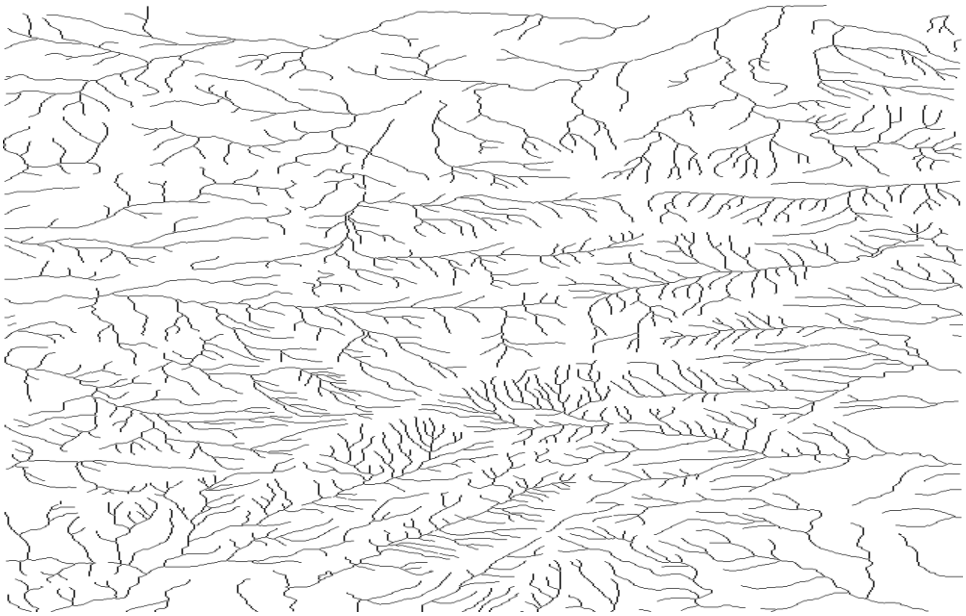

Channel network of Gunung Ledang Region

45

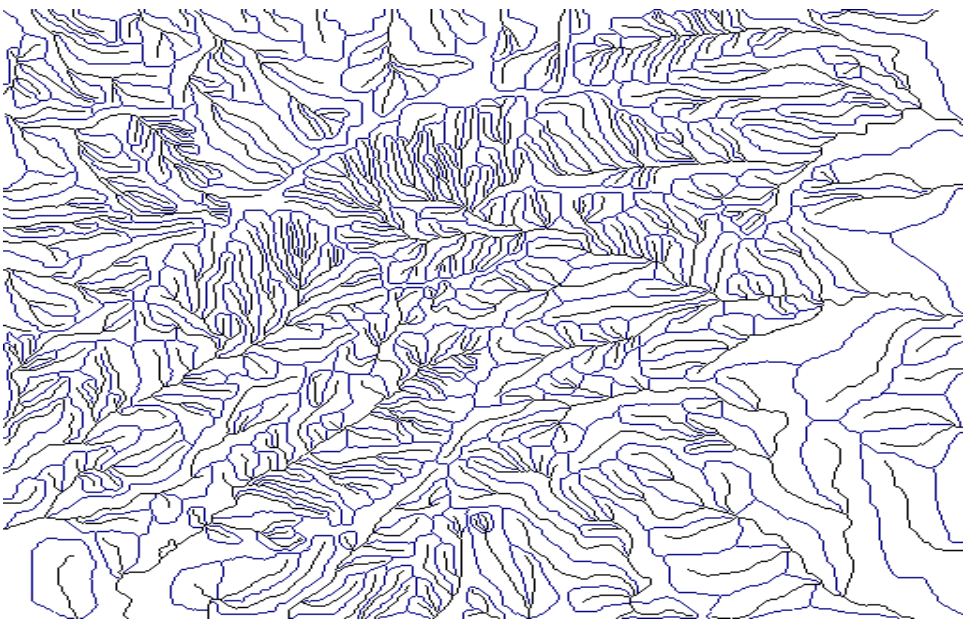

Ridge network of Gunung Ledang Region

46

Networks extraction and their properties

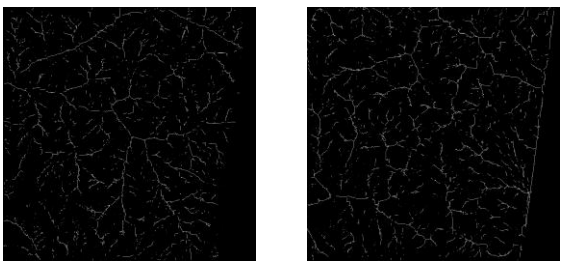

(a) Ridge networks, and (b) channel networks extracted from Cameron Highlands DEM.

47

Networks extraction and their properties

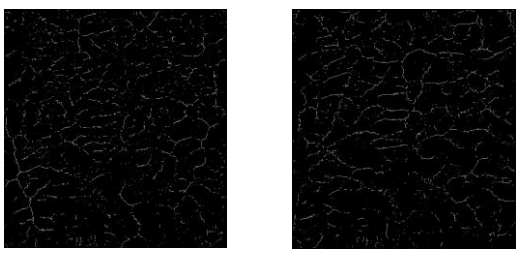

(a) Ridge networks, and (b) channel networks extracted from Petaling DEM.

48

Networks extraction and their properties :Sub-basins delineation

- A drainage basin is defined as an area outlined by a topographic boundary that diverts all runoff, throughflow and groundwater flow to stream networks flowing into a single outlet. The drainage boundary is named as watershed and it divides one basin from another, and separates runoff between them.
- Besides networks extraction, DEM is also a very useful and popular source for watershed extraction and characterisation. In order to delineate sub-basins, flow direction and flow accumulation grids are formed.
- The hydrologic flow is modelled using eight-direction pour point model (Puecker et. al., 1975) as shown in Figure below. The runoff of a pixel in DEM flows towards one of its eight neighbours with the lowest height.
- The slope between the pixel under consideration, and its lowest neighbour has the greatest value. By taking the highest slope for all pixels in terms of the direction towards its lowest neighbour, the flow direction grid is formed.
- Based on the flow direction grid, the total number of contributing grid cells that flow into each “downstream” grid cell is computed to form the flow accumulation grid set.
- Grid cells with large values of flow accumulation are areas of concentrated flow and are identified as stream channels according to the specified flow accumulation threshold. Grid cells with flow accumulation values of zero are topographic highs or ridges, which are the watershed boundaries. Based on these features, the watershed and sub-watershed boundaries are modelled.

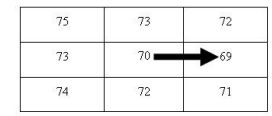

49

Networks extraction and their properties : Sub-basins delineation

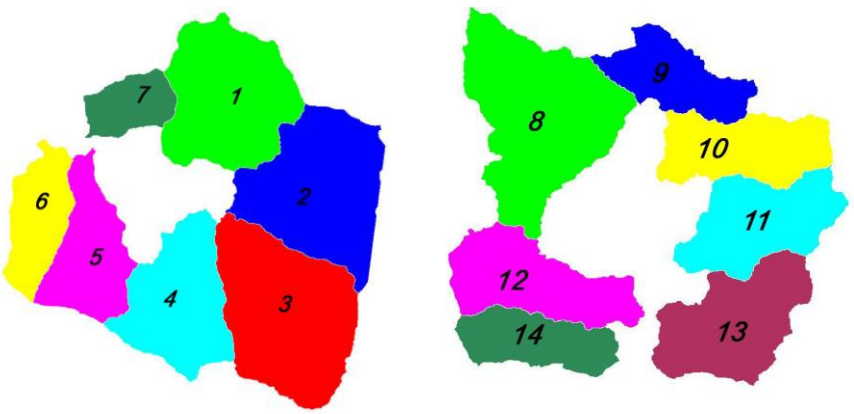

The example of a few sub-basins delineated from Cameron Highlands and Petaling DEM is illustrated in figures above.

50

Decomposed basins and networks

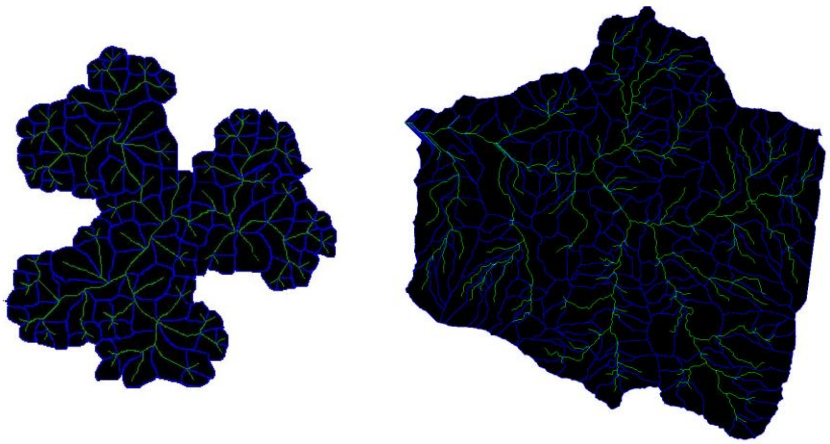

51

Networks extraction and their properties : Networks ordering

- An important quantifiable characteristic of stream networks is related to the hierarchical arrangement of stream channels. Therefore, the first step in drainage basin analyses is the classification of stream orders by using the most common ordering system, i.e. Horton-Strahler's ordering system (Horton, 1945; Strahler, 1957).
- According to this ordering system, the smallest headwater fingertip tributaries with no other tributaries are assigned as first-order stream. When two first-order channels join, a channel segment of order two is formed. Generally, the joint of two *n* order channels produces a segment of order *n*+1.
- Streams of lower order joining a higher order stream do not change the order of the higher stream. Thus, if a second-order stream joins with a third-order stream, it remains a third-order stream.
- When a branch has more than two sub-branches, only the two of highest orders are considered.
- The order of the whole tree is defined to be the order of the root, its lowest-lying branch. It is a measure of the complexity of the tree.
- This ordering system has been found to correlate well with important basin properties in a wide range of environments.

52

Networks extraction and their properties : Networks ordering

This figure shows a sample network classified based on Horton-Strahler's ordering system.

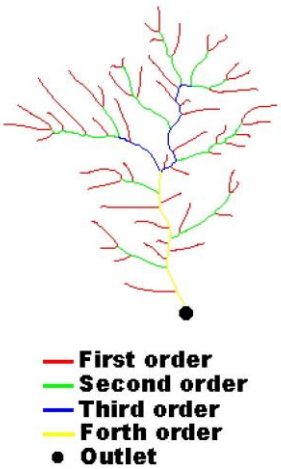

53

Networks extraction and their properties : Networks ordering

Horton-Strahler's ordering system is applied on Cameron Highland channel network.

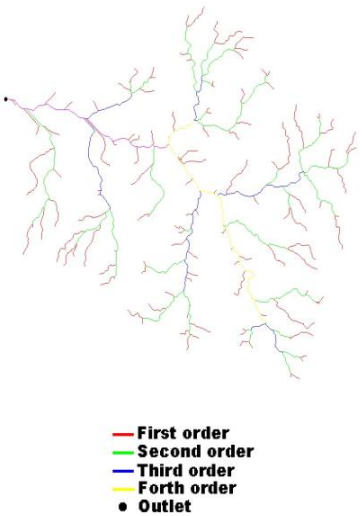

54

Networks extraction and their properties : Morphometry

- There are two main ratios in morphometry, i.e. the bifurcation ratio (R_b) and length ratio (R_l). Consider a tree with order *k*, the stream number of order *i* is given as N_i . Since the order of the whole tree is *k*, then N_k = 1. It is noticeable that the number of stream segments is larger for lower order segment. Bifurcation ratio, R_b is defined as the ratio of the number of streams of a given order to the number in the next higher order.

$$R_b = \frac{N_i}{N_{i+1}}$$

- The bifurcation ratio is not exactly the same for all orders, however it tend to be a constant throughout the series. Since the number of streams within each order decreases with order in a linear fashion, the logarithm of bifurcation ratio can be obtained as the slope of graph, where logarithm value of number of streams is plotted against stream order.
- The length ratio, R_l, is based on the law of stream lengths, where the ratio of the length of streams in successive stream orders is computed. Let L_i be the mean length of streams with order *i*, R_l is defined by equation below,

$$R_l = \frac{L_i}{L_{i-1}}$$

- The law of stream lengths indicates that the length of streams in successive higher stream orders increases by following a geometric relationship. By plotting the logarithm values of stream length as a function of stream order, length ratio can be derived.

55

Reservoir Isolation

♦ The centroids of decomposed zones shown with different colours are connected to form the network with in the reservoir.

♦ This connectivity network is overlaid on stream network that is traced and digitized to convert this whole reservoir catchment into connectivity-like information.

♦ Strahlers ordering scheme is applied to the whole connectivity network using the equation ω = max{i,j,int(1+(1/2)(i+j))} where ω is stream order and it is shown with different colours.

♦ The basic measures such as order-wise lengths, number and mean lengths within this 4th order network are computed.

56

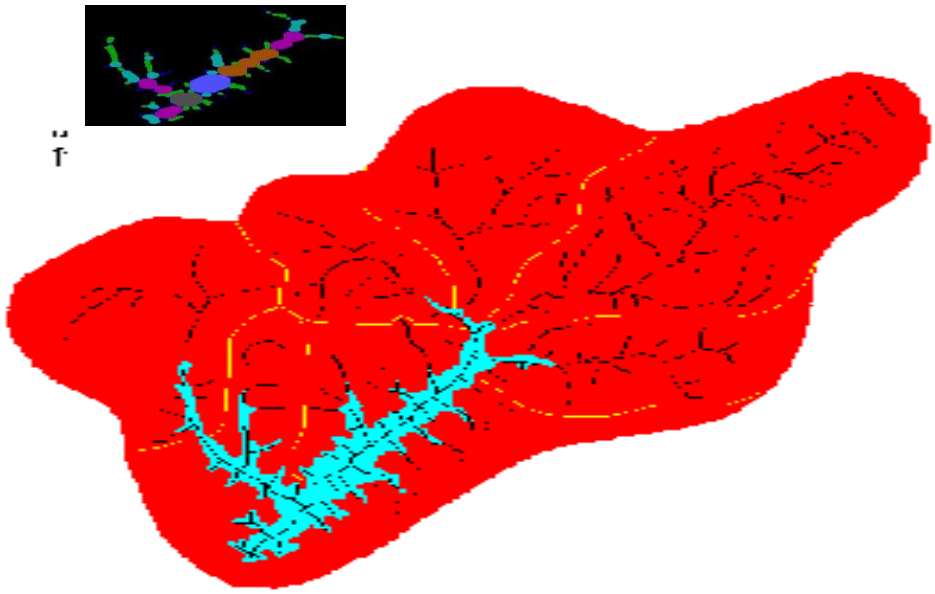

Sub catchments contributing to reservoir catchment

57

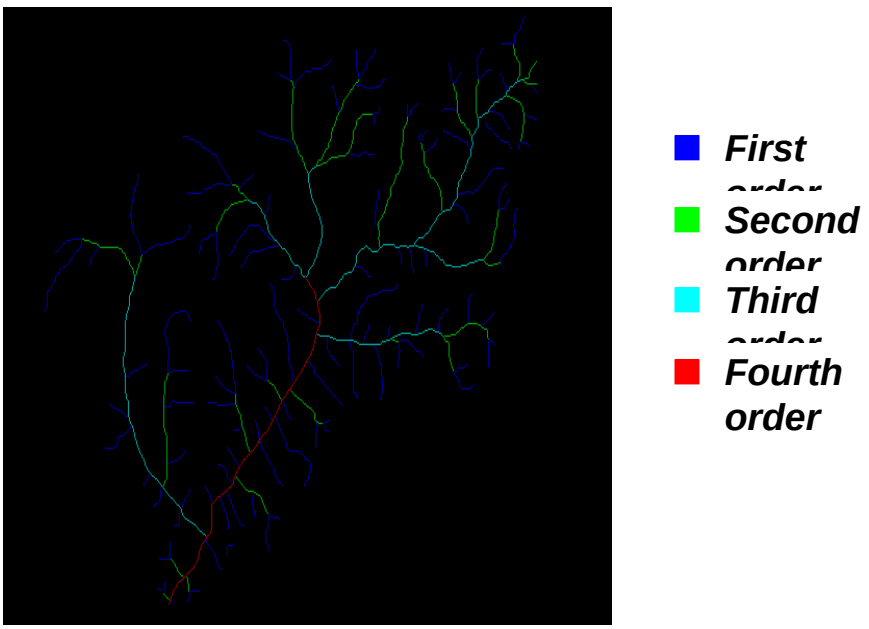

Network with Strahlers ordering technique

58

Morphometric Analysis of network with in the catchment

Number of Orders

1st order segments – 130

2nd order segments – 28

3rd order segments – 6

4th order segments – 1

Mean Lengths

1st order – 0.44

2nd order – 0.82

3rd order - 3

4th order - 6

Order-wise lengths

1st order length – 57

2nd order length – 23

3rd order length – 18

4th order length – 6

Bifurcation ratio

N1/N2 - 4.6

N2/N3 – 4.7

N3/N4 - 6

RB – 5.1

59

Morphometric Analysis of network with in the catchment

Mean Length ratio

L2/L1 - 1.86

L3/L2 – 3.66

L4/L3 – 2

RL – 2.51

♦ The computed ratio of logarithms of bifurcation and mean length ratios of the network yields 1.77, which is the fractal dimension of catchment.

60

Networks extraction and their properties : Morphometry

- Besides these two ratios, the universal similarity of stream network can be shown through Hack's law and Hurst's law as follows:
- Hack's law:

$$L_{\mathrm{mc}} \propto A^{h}$$

where A is the area of basin with main channel length L_{mc}.

- Hurst's law:

$$L_{\perp} \propto L_{\parallel}^{H}$$

where $L_{||}$ and $L_{\perp}$ is the longitudinal length and transverse length respectively.

61

Networks extraction and their properties : Morphometry

	R_b	R_l	h	H	Hypsometric Integral
Basin 1	3.60	2.21	0.5414	0.9714	0.42
Basin 2	4.35	2.25	0.5561	1	0.42
Basin 3	3.31	2.39	0.5612	0.9256	0.46
Basin 4	4.47	3.18	0.5671	0.9506	0.39
Basin 5	3.31	2.16	0.5766	0.9162	0.58
Basin 6	4.00	2.64	0.5746	0.8597	0.49
Basin 7	2.82	2.39	0.5548	0.8950	0.50
Basin 8	5.00	2.58	0.5568	0.9319	0.44
Basin 9	4.00	3.51	0.5828	0.8623	0.51
Basin 10	4.24	3.31	0.5970	0.9019	0.49
Basin 11	4.24	2.97	0.5807	0.8902	0.42
Basin 12	4.80	3.97	0.5844	0.8704	0.38
Basin 13	4.90	3.42	0.5713	0.9116	0.38
Basin 14	3.61	3.39	0.5865	0.8312	0.34

Morphometric ratios and hypsometric integrals for fourteen basins of Cameron Highlands and Petaling regions.

62

Existing allometric power-laws

63

Existing allometric power-laws

- Validation of existing allometric power-laws is carried out by using sub-basins of simulated fractal-DEM and TOPSAR DEM.
- Basic measures such as basin area, basin perimeter, channel length, longitudinal length and transverse length are computed. Allometric power-law relationships are derived among the basic measures of decomposed sub-basins of all orders.
- It is reported that these power-laws are also of universal type as they exhibit similar scaling (power-law) relationships at all scales.
- The results are in good accord with that of natural river basins.

64

Existing allometric power-laws : Decomposed basins and networks

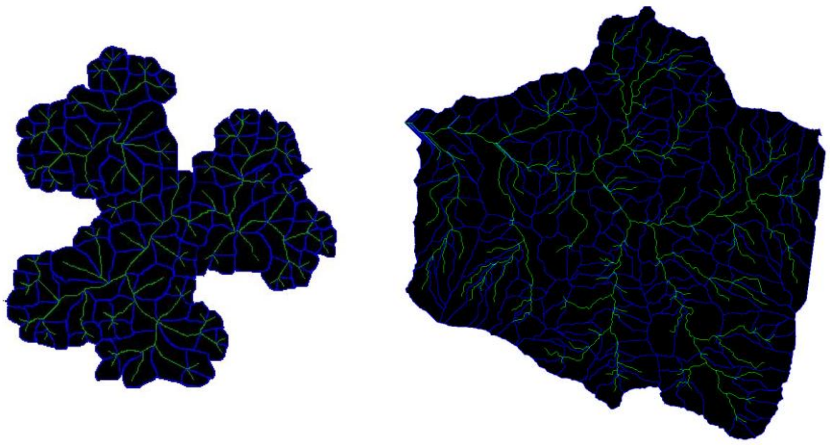

65

Existing allometric power-laws : Decomposed basins and networks

The number of decomposed sub-basins of respective orders from the simulated 6th order F-DEM include

- two 5^{th}
- five 4^{th}
- ten 3^{rd}
- thirty six 2^{nd}, and
- eighty six 1^{st} order basins.

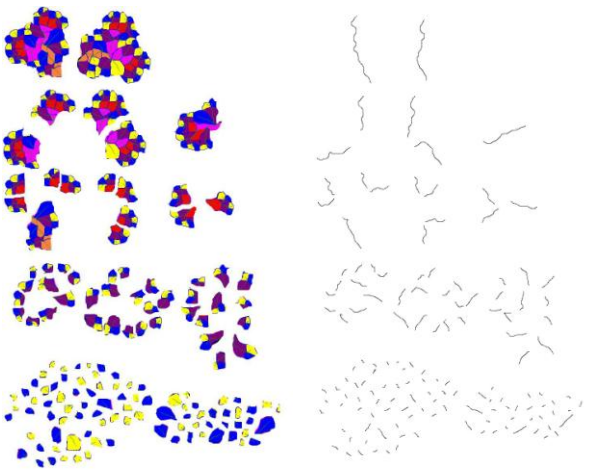

66

Existing allometric power-laws : Decomposed basins and networks



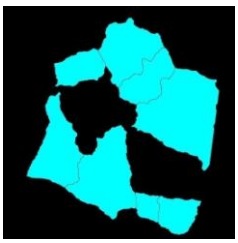

Decomposed sub-basins are
- two 4th
- eight 3rd
- twenty-eight 2nd, and
- one hundred twenty-four 1st

order basins.

67

Existing allometric power-laws : Decomposed basins and networks

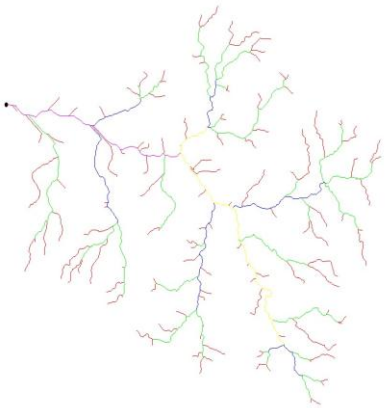

68

Existing allometric power-laws : Basic Measures

Basic measures for a basin, (a) basin area, (b) total channel length, (c) main channel length, (d) basin perimeter, (e) longitudinal length and (f) transverse length.

69

Existing allometric power-laws : Scaling laws

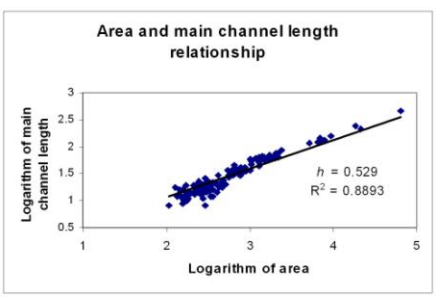

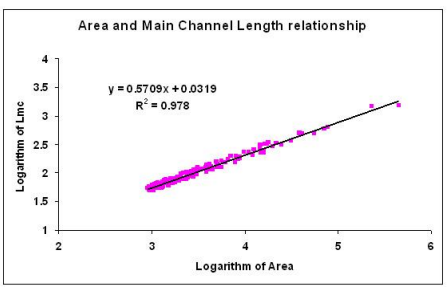

Allometric relationship between main channel length and basin area for all sub-basins of F-DEM and TOPSAR DEM.

70

Existing allometric power-laws : Scaling laws

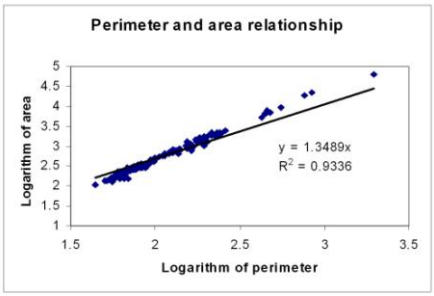

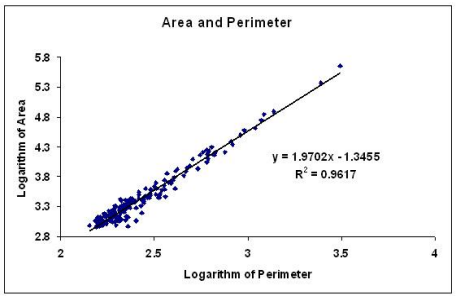

Allometric relationship between area and perimeter for all sub-basins *of* F-DEM and TOPSAR DEM.

71

Existing allometric power-laws : Scaling laws

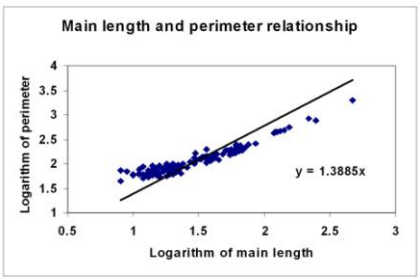

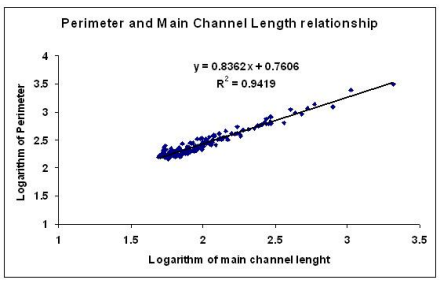

Allometric relationship between perimeter and main channel length for all sub-basins of F-DEM and TOPSAR DEM.

72

Existing allometric power-laws : Scaling laws

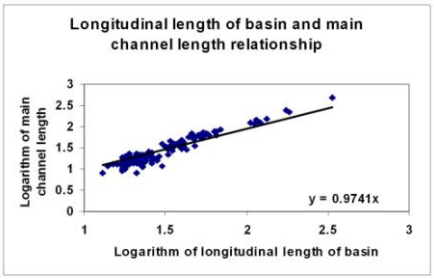

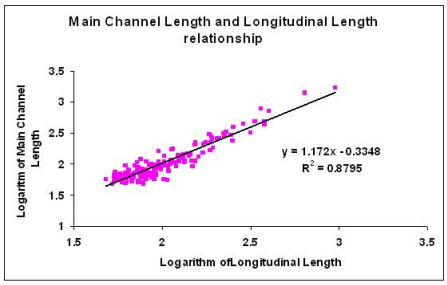

Allometric relationship between L_{ll} and L_{mc} for all sub-basins of F-DEM and TOPSAR DEM.

73

Existing allometric power-laws : Scaling laws

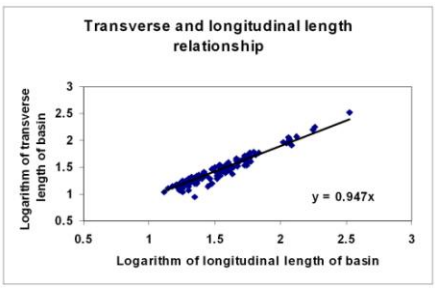

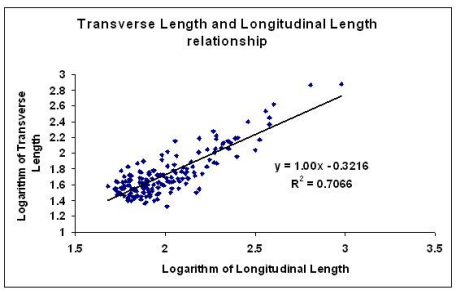

Allometric relationship L_{II} between $L_{\perp}$ and for all sub-basins of F-DEM and TOPSAR DEM.

74

Existing allometric power-laws : Scaling laws

Power-law values among allometric measures of F-DEM

Relations	Notations	For all orders	Basin's order					
			1	2	3	4	5	6
A and L_{mc}	h	0.53	0.502	0.56	0.56	0.55	0.55	0.56
A and P	α	1.35	1.31	1.36	1.41	1.44	1.48	1.46
P and L_{mc}	β	1.39	1.51	1.32	1.28	1.26	1.23	1.23
L_{mc} and L_{ll}	-	0.97	0.92	1.01	1.04	1.03	0.94	0.95
$L_{\perp}$ and L_{ll}	H	0.95	0.94	0.94	0.96	0.98	0.94	0.98
2h	D_{Lmc}	1.06	1.00	1.11	1.11	1.10	1.10	1.12
$2/\alpha$	D_P	1.48	1.53	1.47	1.42	1.39	1.35	1.37
$1+\frac{D_{Lmc}}{1+H}$	-	1.55	1.52	1.57	1.59	1.56	1.57	1.57

75

Existing allometric power-laws : Scaling laws

Power-law exponents among allometric measures of TOPSAR DEM

Relations	Notations	For all orders	Basin's order				
			1	2	3	4	5
A and L_{mc}	h	0.57	0.60	0.57	0.50	0.58	0.56
A and P	α	1.97	1.62	1.78	1.78	1.69	1.62
P and L_{mc}	β	0.84	0.78	0.92	0.88	1.09	1.05
L_{mc} and L_{ll}	-	1.17	0.75	1.00	0.92	1.02	1.08
$L_{\perp}$ and L_{ll}	H	1.00	0.39	0.53	0.68	1.00	0.97
2h	D_{Lmc}	1.14	1.20	1.14	1.00	1.16	1.12
$2/\alpha$	D_P	1.02	1.23	1.12	1.12	1.18	1.23
$1+\frac{D_{Lmc}}{1+H}$	-	1.57	1.86	1.74	1.60	1.58	1.57

76

Existing allometric power-laws : Scaling laws

- Comparisons between our estimates and important allometric power-laws exponnts derived from OCN (optimal channel networks, Maritan et. al., 2002), RSN (random self-similar network (Veitzer and Gupta, 2000) and certain natural river basins.
- Basins of F-DEM and TOPSAR DEM are geomorphologically realistic as OCN,RSN and realistic river basins.

77

Novel scaling relationships between travel-time channel networks, convex hulls and convexity measures

78

Novel scaling relationships

- Network topology and watershed geometry are two important features in terrain characterisation, therefore the length of the travel-time networks and area of the corresponding convex hull are used to derive new scaling exponents.
- Travel-time networks are investigated based on the consideration of the time required for the particle in the fluid to reach the outlet.
- Travel-time networks refer to sequence of networks generated by removing the end-points (extremities) of the original network iteratively.
- Morphological Hit-or-Miss transformation is used in this pruning process - useful in detecting the exact pattern of structuring templates in images.

79

Proposed scaling relationships : Hit-or-Miss Transformation

a. the original set, S and S^c;
b. the templates, B_1;
c. the templates, B_2;
d. the union of B_1 and B_2;
e. the union of morphological erosions of S by B_1 (**bold 1**) and its complementary space (S^c) by B_2 (*italic 1*);
f. the intersect of morphological erosions of S and its complementary space (S^c) by B_1 and B_2, respectively. The intersecting portion is the results of hit-or-miss transformation.

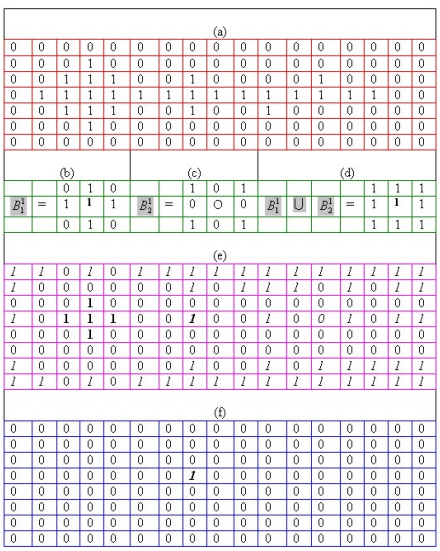

80

Proposed scaling relationships : Travel-time networks

- The process of deleting the end points from the networks is named as pruning.
- To decompose the stream network subsets from *n* = 1 to *N*, structuring template of B_1 and B_2 are decomposed into various subsets, B_n^i where $i = 1,2,...,8$ and $n = 1,2$

- Both structuring templates are disjointed into eight directions. The intersecting portion of eroded *S* and eroded *Sc* by disjointed templates $\{B_1^k\}$ and $\{B_2^k\}$, $k = 1,2,...,8$ respectively are computed to derive pruned version of *S*.
- The X's in the structuring templates signifies the 'don't care' condition – it doesn't matter whether the pixel in that location has a value of 0 or 1.

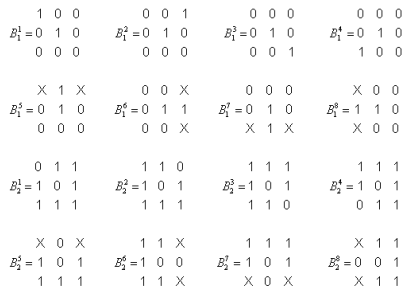

Proposed scaling relationships : Travel-time networks

- Mathematically,
- $S * B = (S \ominus B_1^k) \cap (S^c \ominus B_2^k)$, where $B = B_1^k \oplus B_2^k$
- By subtracting $(S * B)$ from S, a pruned version of *S* is obtained and expressed as
- $S_1 = S \otimes \{B\}$ where, $S \otimes \{B\} = S - (S * B))$
- $\{B\}$ is the sequence of $\{(B_1^1, B_1^2, \cdots, B_1^8), (B_2^1, B_2^2, \cdots, B_2^8)\}$
- After pruning of S in first pass with B_1, the process continue with pruning with B_2 and so on until S is pruned in the last pass with B_8. $S \otimes \{B\} = ((\cdots((S \otimes B^1) \otimes B^2) \cdots) \otimes B^8)$
- The whole process will remove the first-encountered open pixels of S and produce S_1.
- Repeating the same process on S_1 will produce S_2 . The process is repeated until no further changes occur, where the closed outlet is reached.

Proposed scaling relationships : Travel-time networks

Properties of the pruned network:

1. $S = \bigcup_{n=0}^{N-1} (S_n - S_{n+1})$
2. $S_N \subset S_{N-1} \subset \cdots \subset S_2 \subset S_1 \subset S_0 = S$
3. $S, S_1, S_2, \cdots, S_N$ obtained by iterative pruning

83

Proposed scaling relationships : Convex hull

- Convex hull is the smallest convex set that contains all the points of the network.
- Since convex hull represents the basin of network, convex hulls of the sequence travel-time networks are generated.

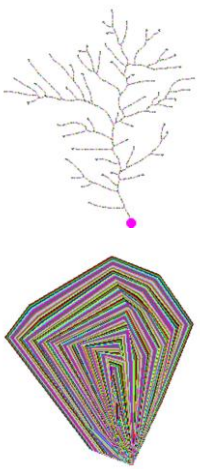

84

Proposed scaling relationships : Convex hull

Half-plane closing-based algorithm (Soille, 2005) is employed to generate convex hulls for these travel-time networks.

The final convex polygon containing all the points of S yields C(S).

85

Proposed scaling relationships : Convexity Measures

- The basic measures are length of networks and areas of convex hulls were computed to estimate the convexity measures of travel-time networks.
- The convexity measure, CM(*S*) of a non-convex shape is defined as the ratio between the areas of Sn and $C(S_n)$. The values of convexity measure range from 0 to 1.
- The rate of change in the areas of S_n is relatively slower than that of $C(S_n)$ for increasing *n*. In channel network, area of *Sn* is equivalent to the length of the total network, $L(S_n)$. Hence, the convexity measures of decreasing $L(S_n)$ and $A[C(S_n)]$converge.
- These measures provide a convergent series, and they are invariant under similarity transformations.
- The upper limit of the convexity measure is attained when the length of the channel network is equal to the area of the convex hull (both being measured by number of pixels).
- This convexity measure of channel networks is similar to drainage density. Drainage density approaching 1 indicates that the channel network possesses space-filling property.

86

Proposed scaling relationships : Pruned network and convex hull

- Images

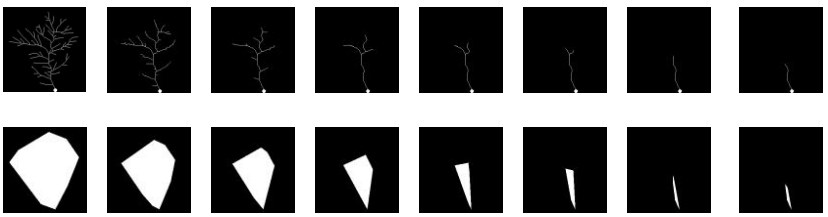

87

Proposed scaling relationships

- Network – pruning – network length = S_n
- Convex hull computed – convex hull area = $C(S_n)$
- Convexity measures, CM = ratio between the areas of S_n and $C(S_n)$.

$$L(S_n) \sim A[C(S_n)]^{\alpha}$$

$$CM(S_n) \sim \frac{1}{L(S_n)^{\beta}}$$

$$CM(S_n) \sim \frac{1}{A[C(S_n)]^{\lambda}}$$

88

Proposed scaling relationships

- Graph of lengths of the sequential pruned networks versus the corresponding areas of convex hulls.

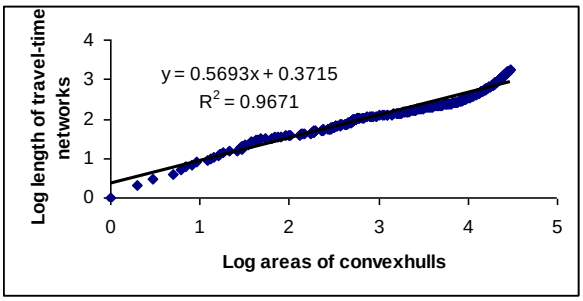

89

Proposed scaling relationships

- Relationship between channel lengths and convexity measures.

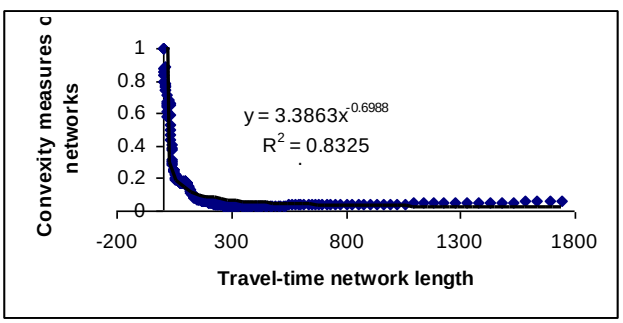

90

Proposed scaling relationships

- Relationship between areas of convex hulls and convex measures.

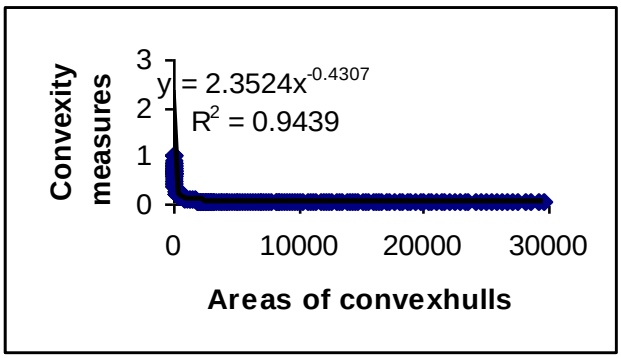

91

Proposed scaling relationships

- Sample basin
- Simulated F-DEM basins
- Cameron basins
- Petaling basins

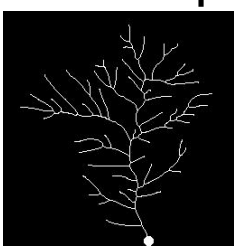

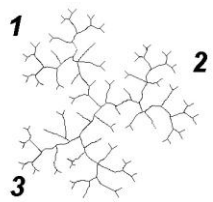

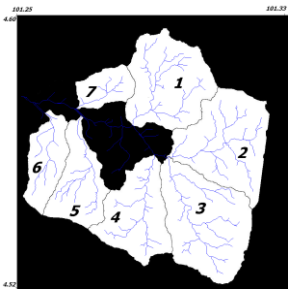

92

Proposed scaling relationships

Network	α, (R^2)	σ, R^2	λ, R^2	R_b	R_l	h	H
Sample	0.5693, (0.9671)	0.6988, (0.8325)	0.4307, (0.9439)	3.84	1.66	-	-
Basin 1 (Cameron)	0.5777, (0.9883)	0.7109, (0.9358)	0.4223, (0.9783)	3.60	2.21	0.5414	0.9714
Basin 2 (Cameron)	0.5774, (0.9925)	0.7189, (0.9586)	0.4226, (0.9861)	4.35	2.25	0.5561	1
Basin 3 (Cameron)	0.5799, (0.9934)	0.7131, (0.963)	0.4201, (0.9875)	3.31	2.39	0.5612	0.9256
Basin 4 (Cameron)	0.5521, (0.9835)	0.7814, (0.92)	0.4479, (0.9752)	4.47	3.18	0.5671	0.9506
Basin 5 (Cameron)	0.5798, (0.9905)	0.7083, (0.9469)	0.4202, (0.982)	3.31	2.16	0.5766	0.9162
Basin 6 (Cameron)	0.5819, (0.9865)	0.6955, (0.925)	0.4181, (0.9743)	4.00	2.64	0.5746	0.8597
Basin 7 (Cameron)	0.5885, (0.9887)	0.68, (0.9348)	0.4115, (0.9772)	2.82	2.39	0.5548	0.895
Basin 1 (Petaling)	0.5462, (0.969)	0.7741, (0.8561)	0.4538, (0.9557)	5.00	2.57	0.5568	0.9319
Basin 2 (Petaling)	0.5393, (0.9899)	0.8357, (0.9532)	0.4607, (0.9863)	4.00	3.51	0.5828	0.8623
Basin 3 (Petaling)	0.5198, (0.9852)	0.8953, (0.9367)	0.4802, (0.9827)	4.24	3.30	0.597	0.9019
Basin 4 (Petaling)	0.5592, (0.9938)	0.7771, (0.9684)	0.4408, (0.99)	4.24	2.96	0.5807	0.8902
Basin 5 (Petaling)	0.5729, (0.9906)	0.729, (0.9492)	0.4271, (0.9832)	4.79	3.96	0.5844	0.8704
Basin 6 (Petaling)	0.5547, (0.9872)	0.7798, (0.937)	0.4453, (0.9804)	4.89	3.42	0.5713	0.9116
Basin 7 (Petaling)	0.6059, (0.9929)	0.6387, (0.9551)	0.3941, (0.9834)	3.60	3.39	0.5865	0.8312

Allometric power-laws between travel-time channel networks, convex hulls, and convexity measures for model network, networks of Hortonian fractal DEM, and networks of fourteen basins of Cameron Highlands and Petaling region.

93

Proposed scaling relationships

- These proposed scaling exponents are shown for basins derived from simulated F-DEM and TOPSAR DEMs.
- These exponents are scale-independent.
- At macroscopic level, these exponents complement with other existing scaling coefficients can be used to identify commonly sharing generic mechanisms in different river basins.

94

Fractal and multiscale analyses of planar geophysical networks

95

Fractal and multiscale analyses of networks

- A new approach of fractal dimension estimation is suggested in this analysis.
- Firstly, multiscale DEMs are generated *via* multiscale opening and closing transformations. The resolution of DEM becomes coarser with increasing cycle of opening/closing transformation.
- Both ridge and channel networks are extracted from these multiscale DEMs.
- A scaling exponent is derived by plotting the length of the network as function of the radius of structuring element employed to generate multiscale DEMs.
- This relationship possesses a linear property on a log-log graph. The exponent value derived from the best fit line is fractal-like scaling exponent.
- The derived fractal dimension is resolution-independent as the networks are extracted from basins of multiple resolutions. As compared to box-counting dimension, which describes the space-filling property of networks, the new proposed fractal dimension complements the existing methods in terrain characterisation.

96

Fractal and multiscale analyses of networks

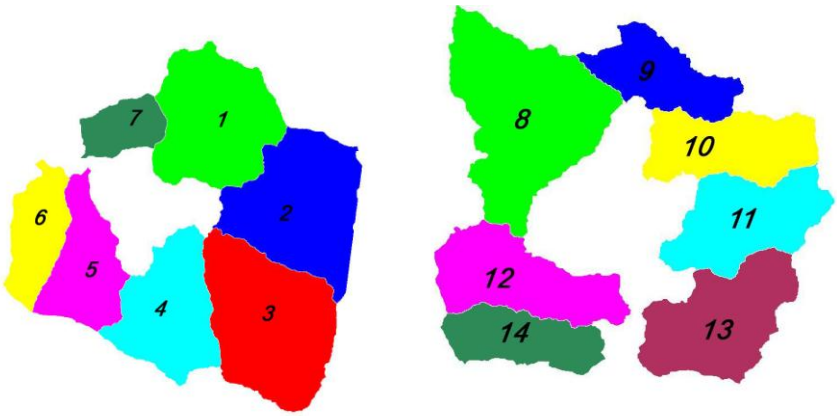

97

Fractal and multiscale analyses of networks

- Morphology Opening and Closing
- Multiscale DEM images (Opening and Closing by square structure element 3X3 to 21X21)

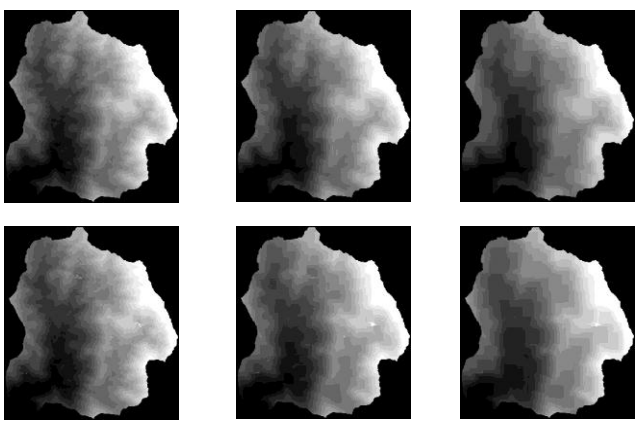

98

Fractal and multiscale analyses of networks : Post processing

- Thresholding
- Thinning
- Ridge

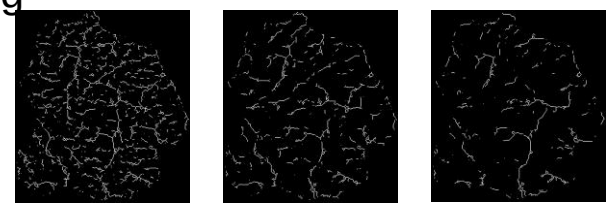

- Channel

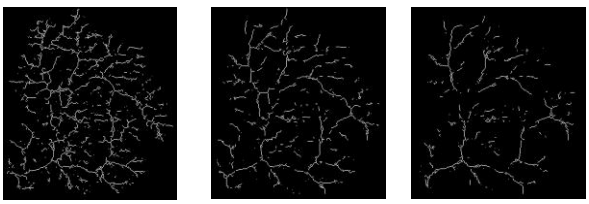

99

Fractal and multiscale analyses of networks : Fractal Dimension

- Graph: Network length vs scale

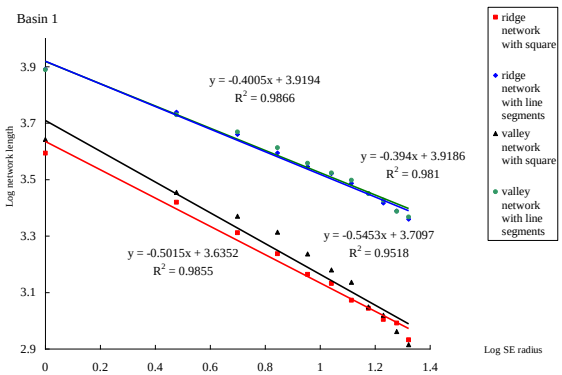

100

Fractal and multiscale analyses of networks : Fractal Dimension

	Network extraction using line segments		Network extraction using square template	
Basin	Fractal dimension derived from ridge network.	Fractal dimension derived from channel network.	Fractal dimension derived from ridge network.	Fractal dimension derived from channel network.
Basin 1	1.4005	1.394	1.5015	1.5453
Basin 2	1.4097	1.4596	1.5184	1.5941
Basin 3	1.4204	1.3883	1.585	1.5926
Basin 4	1.5057	1.4068	1.7092	1.5301
Basin 5	1.4262	1.3402	1.5729	1.6233
Basin 6	1.3656	1.3314	1.5403	1.5412
Basin 7	1.3927	1.3468	1.5271	1.4273
Basin 8	1.3505	1.3688	1.512	1.4442
Basin 9	1.3349	1.3358	1.4251	1.3989
Basin 10	1.3781	1.357	1.5183	1.437
Basin 11	1.3137	1.3072	1.4263	1.3982
Basin 12	1.341	1.3342	1.5228	1.4644
Basin 13	1.299	1.3075	1.452	1.3735
Basin 14	1.3842	1.3367	1.5083	1.4658

101

Fractal and multiscale analyses of networks : Fractal Dimension

- This relationship depicts that similar trends have been followed for both ridge and channel connectivity networks, which shows the duality of both networks. It also describes the scaling properties of the terrain, where the density of the networks decreases as the resolution decreases. This change is due to the fact that the diffuse character of the basin increases as the size of the structuring template increases. This relation can be reversed and estimation of lengths of these networks can be made from coarse scale information.
- The lengths of channel and ridge networks extracted by employing line segment structuring elements are significantly more than that of the networks extracted by convex type of square template.
- The gradients of best fit lines of these plots indicate that the rate of change in the lengths of the networks across multiple resolutions. The rate derived by combination of segment-like structuring elements is slower than that of the networks derived by square element.
- Intricacy of the networks observed for Cameron sub-basins is denser as compared to the intricacy of Petaling networks. In general, hilly terrain possesses higher value of exponent as compared to non-hilly terrain. The reason is the rate of change in the elevation of hilly terrain across resolutions is higher than non-hilly terrain. Relatively, the network intricacies will also change more rapidly for hilly terrain.
- Since the power-law exponent is sensitive to the shape of structuring elements (shape-dependent), its value would be related to the shape and roughness of the terrain. Thus, these power laws can be related to terrain roughness characteristics.
- The analyses of networks extracted by structuring elements of each direction provide new insight to understand the direction-specific terrain complexity.

102

Conclusions

- Two ways of characterising terrain through analysing DEM's are:
  - (i) analysing three-dimensional DEM by considering it as grey-scale image, and
  - (ii) analysing topologically significant unique geophysical networks that could be decomposed from DEMs.
- In the latter case, the decomposed information is in the form of planar sets. Characterisation of terrain using these two mentioned forms is done *via* metric based methods. These methods include morphometry, granulometry, fractal technique and allometry.
- Simulated Hortonian F-DEM, TOPSAR DEM's of Cameron and Petaling regions and the associated geophysical networks are considered as main inputs for these metric based methods. These two regions are chosen because they posses rather contrasting topographic constitutions. The Cameron region possesses high altitude basins, whereas, the Petaling region possesses relatively gentle-slope and rather flat topography.

103

Conclusions (cont)

- Two main relevant features extracted from DEMs are channel and ridge connectivity networks. New algorithms for both ridge and channel networks extraction are developed based on simple morphologic transformations and certain logical operations. The advantage of the algorithms developed over the other existing algorithms is that it can be generalised to any kind of topography irrespective of topographic roughness.
- General allometric relationships between the basic measures derived from channel networks and their corresponding basins. The relationships exhibit remarkable universality scaling attributed that these basins and their associated features follow commonly sharing generic mechanisms in their formation and subsequent spatio-temporal evolution. All these results are in conformity with well-documented literature on the topic.

104

Conclusion (cont)

- From the planar channel network, a causal allometric relationship is proposed. This relationship is between the travel-time network, its corresponding convex hull and convexity measure. A remarkable universal relationship is proposed, and it can further be linked with the involved geophysical processes. The universality constant is highly dependent on basin's general topological and geometric organisation. This new relationship provides potentially valuable insights to further explore links with terrain characteristics, other established allometric relationships and geophysical processes.
- A new approach of fractal dimension estimation is suggested based on length of networks extracted from multiscale DEMs. The derived fractal dimension is resolution-independent as the networks are extracted from basins of multiple resolutions.
- Regions with similar topological quantities and scaling exponents would have different roughness property. An alternative approach is proposed to quantify the terrains in terms of shape dependent measures, i.e. granulometric approach. These measures are scale-invariant but shape-dependent.

105

Conclusions (cont)

In summary, the key findings of this project include:

a. Verification of morphometry property and basic allometry power law on TOPSAR DEMs and simulated F-DEM.
b. Algorithm development for travel-time networks generation based on morphological pruning process.
c. Algorithm development for convex-hull construction for the travel-time networks.
d. Proposed convexity measures based on the length of travel-time networks and the area of corresponding convex hulls.
e. Proposed new power (scaling) laws on travel-time network length, convex hull area and the derived convexity measures.
f. Channel and ridge networks extraction from grey-scale DEM using morphological opening/erosion and closing/dilation respectively.
g. Proposed line segments in 4-direction as structuring element for networks extraction as they follow the networks pattern.
h. Proposed fractal dimension estimated based on the network length across multiple resolutions (i.e. multiscale DEMs).
i. Proposed average size and average roughness calculated for DEM of different regions and different sub-basins.

106

References

- Horton, R. E. (1945). Erosional development of stream and their drainage basin: hydrological approach to quantitative morphology, Bulletin of the Geophysical Society of America, 56, pp. 275-370.
- Langbein, W. B. (1947). Topographic characteristics of drainage basins, U.S. Geological Survey Professional Paper. 968-C, pp. 125-157.
- Strahler, A. N. (1952). Hypsometric (area-altitude) analysis of erosional topography: Bulletin Geological Society of America,v. 63, no. II, pp. 1117-1141.
- Strahler, A. N. (1957). Quantitative analysis of watershed geomorphology. EOS Transactions of the American Geophysical Union, 38(6):913–920.
- Strahler, A. N. (1964). Quantitative geomorphology of drainage basins and channel networks, In Handbook of applied Hydrology (ed. V. T. Chow), New York, McGraw Hill Book Co., Section 4, pp. 4-39 - 4-76.
- Barbera, P. L. and Rosso, R. (1989). On the fractal dimension of stream networks, Water Resources Research, 25(4):735–741.
- Tarboton, D. G., Bras, R. L. and Rodrýguez-Iturbe, I. (1990). Comment on "On the fractal dimension of stream networks" by Paolo La Barbera and Renzo Rosso. Water Resources Research, 26(9):2243–4.
- Maritan, A., Coloairi, F., Flammini, A., Cieplak, M., and Banavar, J. R. (1996). Universality classes of optimal channel networks. Science, 272, 984.
- Maritan, A., R. Rigon, J. R. Banavar, and A. Rinaldo (2002). Network allometry, Geophysical Research Letters, 29(11), p. 1508-1511.
- Rodriguez-Iturbe, I. and Rinaldo, A. (1997). Fractal River Basins: Chance and Self-organization, Cambridge University Press, Cambridge.
- Mandelbrot, B. B. (1982). The Fractal Geometry of Nature. Freeman, San Francisco.
- Turcotte, D. L. (1997). Fractals in Geology and Geophysics, Cambridge University Press, Cambridge.
- Matheron, G. (1975). Random Sets and Integral Geometry, John Wiley Hoboekn, New Jersey.
- Serra, J. (1982), Image Analysis and Mathematical Morphology, Academic Press, London.
- Peucker, T. K. and Douglas, D. H. (1975). Detection of surface-specific points by local parellel processing of discrete terrain elevation data, Computer Vision, Graphics and Image Processing, 4, p. 375-387.
- Veitzer, S. A. and Gupta, V. K., (2000). Random self-similar river networks and derivations of generalized Horton laws in terms of statistical simple scaling, Water Resources Research, Volume 36 (4), 1033-1048.

107

Thank You

Q & A

108

Acknowledgments: Grateful to collaborators, mentors, reviewers, examiners, and doctoral students—Prof. S. V. L. N. Rao, Prof. B. S. P. Rao, Dr. M. Venu, Mr. Gandhi, Dr. Srinivas, Dr. Radhakrishnan, Dr. Lea Tien Tay, Dr. Chockalingam, Dr. Lim Sin Liang, Dr. Teo Lay Lian, Prof. Jean Serra, Prof. Gabor Korvin, Prof. Arthur Cracknell, Prof. Deekshatulu, Prof. Philippos Pomonis, Prof. Peter Atkinson, Prof. Hien-Teik Chuah and several others.